J. Fluid Mech. (1971), *vol.* 48, *part* 4, *pp.* 771–789
Printed in Great Britain

Calculation of the steady flow past a sphere at low and moderate Reynolds numbers

By S. C. R. DENNIS AND J. D. A. WALKER

Department of Applied Mathematics,
University of Western Ontario,
London, Canada

(Received 24 August 1970 and in revised form 17 March 1971)

The steady axially symmetric incompressible flow past a sphere is investigated for Reynolds numbers, based on the sphere diameter, in the range 0·1 to 40. The formulation is a semi-analytical one whereby the flow variables are expanded as series of Legendre functions, hence reducing the equations of motion to ordinary differential equations. The ordinary differential equations are solved by numerical methods. Only a finite number of these equations can be solved, corresponding to an approximation obtained by truncating the Legendre series at some stage. More terms of the series are required as R increases and the present calculations were terminated at $R = 40$. The calculated drag coefficient is compared with the results of previous investigations and with experimental data. The Reynolds number at which separation first occurs is estimated as 20·5.

1. Introduction

The problem investigated is that of steady incompressible axially symmetric viscous flow past a sphere in a uniform stream. Previous numerical solutions of this problem have been given by Kawaguti (1950) at $R = 20$, Lister (1953) at $R = 0, 1, 10, 20$ and by Jenson (1959) at $R = 5, 10, 20, 40$. Here, R is the Reynolds number based on the sphere diameter. These solutions were carried out by applying relaxation methods directly to the governing equations for the vorticity and axially symmetric stream function. A Fourier expansion for the flow variables was used to solve the problem for a wide range of Reynolds numbers by Dennis & Walker (1964). Numerical solutions were given by Hamielec, Hoffman & Ross (1967), Le Clair, Hamielec & Pruppacher (1970) and Pruppacher, Le Clair & Hamielec (1970) using methods similar to those of Jenson, but with finer grid sizes. Finally, Rimon & Cheng (1969) obtained steady solutions by impulsively starting a sphere from rest with uniform velocity and using a time-dependent integration to carry the solution to steady state.

There are also a number of experimental and analytical treatments of this problem. The earlier experimental measurements of the drag on a sphere have been described by Castleman (1926), Goldstein (1938, p. 16), Perry (1950, p. 1018) and Schlichting (1960, p. 16). The recent experimental work of Maxworthy (1965), Pruppacher & Steinberger (1968), Beard & Pruppacher (1969) and Le Clair,

Hamielec & Pruppacher (1970) has suggested that the earlier results are inaccurate. One of the objects of these recent experimental investigations was to check the range of usefulness of expressions for the drag obtained from theoretical treatments of the problem at low Reynolds numbers. Van Dyke (1964*b*, pp. 149–165) has described the theories at low Reynolds numbers for both a circular cylinder and a sphere. A more recent contribution for a sphere, in which the work of Proudman & Pearson (1957) based on matched asymptotic expansions has been further extended, is given by Chester & Breach (1969). Experimental and theoretical investigations of the length of the separated wake region behind the sphere also exist. The dependence of this quantity on Reynolds number has been measured experimentally by Taneda (1956), and a theoretical estimate based on low Reynolds number theory has been illustrated by Van Dyke (1964*b*, p. 159).

One of the objects of obtaining numerical solutions is that some check may be obtained on the experimental and theoretical results. In the previous numerical work there is little detail for very small values of R and discrepancies exist between a number of the results given. In the present paper an attempt to obtain accurate solutions over the range $R = 0{\cdot}1$ to 40 is made using an application of the method of series truncation. A recent paper by Underwood (1969) has applied the series truncation method proposed by Van Dyke (1964*a*, 1965) to calculate the steady flow past a circular cylinder for Reynolds numbers up to 10. The main method used by Underwood (1969) is to expand the stream function as a Fourier series in the polar angle θ, with functional coefficients in the radial variable. The series is substituted in the Navier–Stokes equations and truncated by putting all functional coefficients after a certain stage in the series equal to zero. This gives a finite set of ordinary differential equations to be solved for the functional coefficients. These are solved numerically and the number of equations to be solved depends upon the number of terms retained in the truncated series. A similar method can be used to solve the sphere problem, by employing series of Legendre functions in place of Fourier series.

The problem is expressed in terms of the usual pair of simultaneous equations for the stream function and vorticity written in terms of the co-ordinates (ξ, θ), where $\xi = \log(r/a)$, a is the radius of the sphere centred at the origin, and (r, θ) are polar co-ordinates in a plane through the axis of the sphere. The uniform stream is in the direction $\theta = 0$. The stream function and vorticity are expanded in series of Legendre functions of argument $z = \cos\theta$ with functional coefficients in the variable ξ. When these series are substituted in the governing equations, two sets of second-order ordinary differential equations result. These are truncated and solved numerically. The approach is different in some respects from the treatment of the circular cylinder given by Underwood (1969) who solved a single set of fourth-order differential equations. The method of utilizing the boundary conditions is also different. Calculations have been carried out for

$$R = 0{\cdot}1\,(0{\cdot}1)\,1, 5, 10, 20 \quad \text{and} \quad 40.$$

The results up to $R = 1$ are compared with the theories at low Reynolds numbers and the whole range of results is compared with experimental observations and with other numerical calculations.

2. Analysis

The equation of continuity is satisfied by introducing the dimensionless stream function $\psi(\xi, \theta)$ defined by the equations

$$u = \frac{e^{-2\xi}}{\sin\theta}\frac{\partial\psi}{\partial\theta}, \quad v = -\frac{e^{-2\xi}}{\sin\theta}\frac{\partial\psi}{\partial\xi}, \tag{1}$$

where (u, v) are the dimensionless radial and transverse components of velocity obtained by dividing the corresponding dimensional components by the stream velocity U_∞. The other dependent variable to be used is the dimensionless vorticity $\zeta(\xi, \theta)$ defined by the equation

$$e^{\xi}\zeta = \frac{\partial v}{\partial\xi} + v - \frac{\partial u}{\partial\theta}. \tag{2}$$

The equations satisfied by ψ and ζ are then

$$\frac{\partial^2\psi}{\partial\xi^2} - \frac{\partial\psi}{\partial\xi} + \sin\theta\frac{\partial}{\partial\theta}\left(\frac{1}{\sin\theta}\frac{\partial\psi}{\partial\theta}\right) + \sin\theta\, e^{3\xi}\zeta = 0, \tag{3}$$

and

$$\frac{\partial^2\zeta}{\partial\xi^2} + \frac{\partial\zeta}{\partial\xi} + \cot\theta\frac{\partial\zeta}{\partial\theta} + \frac{\partial^2\zeta}{\partial\theta^2} - \frac{\zeta}{\sin^2\theta} = \tfrac{1}{2}Re^{\xi}\left(u\frac{\partial\zeta}{\partial\xi} + v\frac{\partial\zeta}{\partial\theta} - u\zeta - v\zeta\cot\theta\right), \tag{4}$$

where $R = 2aU_\infty/\nu$ is the Reynolds number, ν being the coefficient of kinematical viscosity. The boundary conditions to be satisfied are

$$\psi = \partial\psi/\partial\xi = 0, \quad \text{when} \quad \xi = 0, \tag{5}$$

$$\psi \sim \tfrac{1}{2}e^{2\xi}\sin^2\theta \quad \text{as} \quad \xi \to \infty. \tag{6}$$

Expansions for ψ and ζ are now assumed in the respective forms

$$\psi = e^{\frac{1}{2}\xi}\sum_{n=1}^{\infty} f_n(\xi)\int_z^1 P_n(t)\,dt, \tag{7}$$

$$\zeta = \sum_{n=1}^{\infty} g_n(\xi)P_n^{(1)}(z), \tag{8}$$

where $P_n(z)$ and $P_n^{(1)}(z)$ are, respectively, the Legendre and first associated Legendre polynomials of order n. Substitution of (7) and (8) in (3) gives

$$f_n'' - (n+\tfrac{1}{2})^2 f_n = n(n+1)e^{\frac{5}{2}\xi}g_n, \tag{9}$$

where primes denote differentiation with respect to ξ. The boundary conditions become

$$f_n(0) = f_n'(0) = 0, \tag{10}$$

$$f_n \sim e^{\frac{3}{2}\xi}\delta_n, \quad \text{as} \quad \xi \to \infty, \tag{11}$$

where $\delta_1 = 1$ and $\delta_n = 0$ if $n \neq 1$. It may be noted that, by integration of (9),

$$f_n' + (n+\tfrac{1}{2})f_n - n(n+1)\,e^{(n+\frac{1}{2})\xi}\int_0^{\xi} e^{-(n-2)t}g_n(t)\,dt = 0, \tag{12}$$

where the constant of integration has been adjusted to satisfy the conditions (10). The condition (11) then implies that

$$\int_0^{\infty} e^{-(n-2)\xi}g_n(\xi)\,d\xi = \tfrac{3}{2}\delta_n. \tag{13}$$

This condition is used in the numerical procedure in a manner to be described. Effectively it replaces the condition (11), which is not required further.

The velocity components (u, v) can be obtained in the form of series by substituting the series (7) into (1). If the resulting expressions are substituted into (4) along with (8), it is found by standard methods of orthogonal functions that (4) can be expressed as the set of ordinary differential equations

$$g_n'' + (1 - A_n)g_n' - \{n(n+1) + B_n\}g_n = S_n. \tag{14}$$

The quantities $A_n(\xi)$, $B_n(\xi)$ and $S_n(\xi)$ can all be evaluated by manipulation of Legendre functions and only the final results will be given. It is found that

$$A_n(\xi) = \tfrac{1}{2}Re^{-\frac{1}{2}\xi} \sum_{j=1}^{\infty} \alpha_{2j,n}^n f_{2j}, \tag{15}$$

$$B_n(\xi) = \tfrac{1}{2}Re^{-\frac{1}{2}\xi} \sum_{j=1}^{\infty} \beta_{2j,n}^n (f_{2j}' + \tfrac{1}{2}f_{2j}) - A_n(\xi), \tag{16}$$

and

$$S_n(\xi) = \tfrac{1}{2}Re^{-\frac{1}{2}\xi} \sum_{i=1}^{\infty} \sum_{\substack{j=1 \\ j+n}}^{\infty} [\alpha_{i,j}^n f_i(g_j' - g_j) + \beta_{i,j}^n (f_i' + \tfrac{1}{2}f_i)g_j]. \tag{17}$$

The constants $\alpha_{i,j}^n$ and $\beta_{i,j}^n$ are derived from the integrals of three associated Legendre functions and may be shown to be given by

$$\alpha_{i,j}^n = \frac{-(2n+1)}{[n(n+1)]^{\frac{1}{2}}} [j(j+1)]^{\frac{1}{2}} \begin{pmatrix} n & i & j \\ -1 & 0 & 1 \end{pmatrix} \begin{pmatrix} n & i & j \\ 0 & 0 & 0 \end{pmatrix}, \tag{18}$$

$$\beta_{i,j}^n = \frac{2n+1}{[n(n+1)]^{\frac{1}{2}}} \left[\frac{j(j^2-1)(j+2)}{i(i+1)}\right]^{\frac{1}{2}} \begin{pmatrix} n & i & j \\ -1 & -1 & 2 \end{pmatrix} \begin{pmatrix} n & i & j \\ 0 & 0 & 0 \end{pmatrix}, \tag{19}$$

where

$$\begin{pmatrix} j_1 & j_2 & j_3 \\ m_1 & m_2 & m_3 \end{pmatrix}$$

are the 3-j symbols. A table of the quantities defined by (18) and (19) and the algorithm to compute them numerically is given by Rotenberg, Bivins, Metropolis & Wooten (1959). Talman (1968) has given a detailed account of the theory underlying their use with Legendre functions.

It is seen that the equations (14) are a set of simultaneous equations which are homogeneous in the functions $g_n(\xi)$ with coefficients which can be calculated numerically from the functions $f_n(\xi)$. The theoretical problem is to solve these equations simultaneously with the set of equations (9). The solutions must satisfy the conditions (10) and (13). Also it may be shown either from Oseen's (1910) approximate solution, which is quoted by Batchelor (1967, p. 241) or from the asymptotic solutions of Walker (1968) that

$$g_n(\xi) \sim D_n e^{-3\xi}, \quad \text{as} \quad \xi \to \infty, \tag{20}$$

where D_n is a constant. A truncation of order n_0 is defined by solving the $2n_0$ second-order differential equations obtained by putting all functions with subscripts greater than n_0 equal to zero in (9) and (14). Numerical solutions are obtained by an iterative procedure and it remains only to describe brief details of the numerical methods which have been used. The set of equations (14) may be termed the vorticity equations. A given solution $g_n(\xi)$ is termed the nth mode.

3. Numerical methods

Each vorticity equation is solved as a boundary-value problem. In accordance with (20) it is assumed that

$$g_n(l) = e^{-3h} g_n(l-h) \quad (n = 1, 2, \ldots, n_0), \tag{21}$$

where l is some sufficiently large value of ξ and h is the step size. The other condition to be satisfied by $g_n(\xi)$ is (13), and this is utilized as follows. Let $G_n(\xi)$ be a solution of (14) which satisfies $G_n(l) = e^{-3h} G_n(l-h)$ and also some arbitrarily imposed value at $\xi = 0$, say $G_n(0) = 1$. Also let $H_n(\xi)$ be a solution of the equation obtained by putting $S_n(\xi) = 0$ in (14) which satisfies the condition $H_n(l) = e^{-3h} H_n(l-h)$ together with an arbitrarily imposed condition, say $H_n(0) = 1$, at $\xi = 0$. Then the function

$$g_n(\xi) = G_n(\xi) + C H_n(\xi) \tag{22}$$

satisfies both (14) and (21). Equation (22) is now multiplied by $e^{-(n-2)\xi}$ and integrated from $\xi = 0$ to $\xi = \infty$, assuming that G_n and H_n behave in the same way as g_n in equation (20) from $\xi = l$ to $\xi = \infty$. Since $g_n(\xi)$ must satisfy (13), the constant C and hence the required $g_n(\xi)$ is determined.

Central differences are used to approximate the derivatives in (14) in obtaining the numerical solutions. We use the Southwell notation for grid points, in which the subscripts 3, 0, 1 denote function values at the points $\xi = \xi_0 - h$, $\xi = \xi_0$ and $\xi = \xi_0 + h$, where ξ_0 is a typical point and h is the grid size. For convenience, the subscript n in (14) is suppressed and the finite-difference approximation at the point $\xi = \xi_0$ can be written

$$g_1 - 2g_0 + g_3 + \tfrac{1}{2}h(1 - A_0)(g_1 - g_3) - h^2\{n(n+1) + B_0\} g_0 - h^2 S_0 = 0. \tag{23}$$

This defines a tridiagonal matrix problem of the form

$$a g_0 + b g_1 + c g_3 = d, \tag{24}$$

where

$$\begin{aligned} a &= -2 - h^2 n(n+1) - h^2 B_0, \\ b &= 1 + \tfrac{1}{2}h(1 - A_0), \\ c &= 2 - b, \\ d &= h^2 S_0. \end{aligned}$$

Approximations to a, b, c and d are known at every grid point during the course of a general iterative method of solution, and the matrix problem defined by (24) is solved using the direct method described by Rosser (1967).

The equations (9) are of the general form

$$f'' - k^2 f = F(\xi) \tag{25}$$

and each has an associated pair of initial conditions $f(0) = f'(0) = 0$ in accordance with (10). A numerical method of solving (25) which is both stable and accurate has been developed by Dennis & Chang (1969) for the case when k is an integer. Since the method is equally applicable when k is any constant, it is used in the present case. Briefly, the technique is to introduce functions

$$r = f' - kf, \quad s = f' + kf,$$

which must therefore satisfy the equations

$$r' + kr = F, \quad s' - ks = F \tag{26}$$

with $r(0) = s(0) = 0$. The first of equations (26) is integrated by a stable step-by-step method in the direction of increasing ξ. The same stable method may be applied to integrate the second of (26) backward from $\xi = l$ to $\xi = 0$. It may be shown by relatively minor modifications of the work of Dennis & Chang (1969) that as long as the condition (13) has been satisfied it is possible to calculate a value for $s(l)$ to initiate the backward integration, and a check on the calculation is provided by the fact that $s(0)$ must come out to be approximately zero. Formulae of integration which lead to very accurate numerical solutions have been given by Dennis & Chang (1969).

For a truncation of given order, the truncated sets of equations (9) and (14) are solved by means of an iterative procedure. A set of iterated solutions

$$\{g_n^{(j)}(\xi) \quad (n = 1, 2, \ldots, n_0)\} \quad (j = 1, 2, 3, \ldots),$$

is obtained from equation (14), together with a corresponding set of solutions of (9), by the following process. Suppose that the iterate with superscript j has been completed. The equations (14) are now solved sequentially from $n = 1$ to n_0. Before each equation is solved, the data for the grid values of a, b, c and d which is required in (24) is calculated from the most recently available information. As each new mode is determined it gives a solution which we may denote by $g_n^{(j+\frac{1}{2})}(\xi)$. The components of the iterate with superscript $j+1$ are then defined by taking the weighted average

$$g_n^{(j+1)}(\xi) = K g_n^{(j+\frac{1}{2})}(\xi) + (1-K) g_n^{(j)}(\xi), \tag{27}$$

where $0 < K \leqslant 1$. Before proceeding to the next value of n, the new mode calculated from (27) is used to obtain a corresponding function $f_n^{(j+1)}(\xi)$ from (9). Finally, when $n = n_0$ the $(j+1)$th iterate is complete and the procedure is repeated until, ultimately, convergence is reached. This is decided by the test

$$|g_n^{(j+1)}(0) - g_n^{(j)}(0)| < \epsilon, \quad \text{for all} \quad n \leqslant n_0, \tag{28}$$

where ϵ is some pre-assigned tolerance. This condition is quite adequate, since it has been verified that convergence on the boundary of the sphere only occurs when convergence throughout the whole field has taken place.

R	h	l	r_∞/a	K	ϵ	n_0
$R \leqslant 1$	0·0245	4·9	134·2	0·05	10^{-5}	6
5	0·0245	4·9	134·2	0·05	10^{-5}	14
10	0·0245	4·9	134·2	0·025	10^{-4}	16
20	0·025	5·0	148·4	0·01	10^{-4}	16
40	0·025	5·0	148·4	0·0075	10^{-4}	20

TABLE 1. Parameters of calculations

The averaging process described by (27) has been found to be necessary to achieve convergence of the iterative procedure. The constant K is a parameter of

the solution. If the iterations are found to be divergent, the parameter K may be reduced until convergence results. The other main parameters are the grid size h, the quantity l defining the maximum value of ξ to which the numerical solutions extend, and the maximum number of modes n_0 used in a given truncation. The effect on the computed solutions of varying all these parameters was considered. As a result of the experience obtained by varying the parameters, the final results presented in the next section are based on the parameters shown in table 1. The quantity r_∞/a is the dimensionless polar distance corresponding to $\xi = l$. The maximum number of modes used was based on a balance between the considerations of obtaining physical properties of reasonable accuracy without an unreasonable amount of computation. Some evidence on the effect of truncating the series is given in the final section.

4. Calculated results

The drag on the sphere and the surface pressure distribution can be calculated from a knowledge of $g_n(0)$ and $g_n'(0)$. These coefficients are given for the first eight modes in tables 2 and 3, respectively. The results are based on solutions obtained using the number of modes given in table 1. Values of $g_n(0)$ for higher modes are less than 10^{-4}. The drag coefficient C_D is defined by the equation

$$C_D = D/(\pi\rho U_\infty^2 a^2),$$

R	$g_1(0)$	$g_2(0)$	$g_3(0)$	$g_4(0)$	$g_5(0)$	$g_6(0)$	$g_7(0)$	$g_8(0)$
0·1	1·5263	−0·0123	—	—	—	—	—	—
0·2	1·5504	−0·0241	—	—	—	—	—	—
0·5	1·6149	−0·0573	−0·0002	—	—	—	—	—
0·8	1·6749	−0·0885	−0·0004	—	—	—	—	—
1	1·7126	−0·1082	−0·0005	—	—	—	—	—
5	2·2205	−0·4116	−0·0011	0·00003	−0·0001	—	—	—
10	2·6764	−0·7075	0·0053	0·0014	−0·0004	−0·0002	—	—
20	3·2008	−1·1185	0·0229	0·0072	−0·0009	−0·0009	−0·0002	—
40	4·0224	−1·7863	0·0609	0·0304	−0·0035	−0·0038	−0·0012	−0·0003

TABLE 2. Vorticity modes on the surface of the sphere

R	$g_1'(0)$	$g_2'(0)$	$g_3'(0)$	$g_4'(0)$	$g_5'(0)$	$g_6'(0)$	$g_7'(0)$	$g_8'(0)$
0·1	−3·0526	0·0402	—	—	—	—	—	—
0·2	−3·1010	0·0789	—	—	—	—	—	—
0·5	−3·2317	0·1898	−0·0001	—	—	—	—	—
0·8	−3·3544	0·2961	−0·0006	0·0001	—	—	—	—
1	−3·4321	0·3646	−0·0012	0·0001	—	—	—	—
5	−4·5380	1·5237	−0·0585	0·0019	0·0011	0·0002	—	—
10	−5·6202	2·8459	−0·2313	0·0017	0·0055	0·0013	0·0002	—
20	−7·0378	5·0255	−0·6890	−0·0112	0·0214	0·0076	0·0014	0·0003
40	−9·5352	9·3083	−1·9251	−0·0905	0·1038	0·0353	0·0083	0·0029

TABLE 3. Vorticity mode derivatives on the surface of the sphere

where D is the total drag on the sphere and ρ is the density of the fluid. The coefficient is composed of two parts due to the friction and pressure drag, respectively. The friction drag coefficient is given by

$$C_f = -\frac{4}{R}\int_0^\pi \zeta(0,\theta)\sin^2\theta\, d\theta,$$

and if the series (8) is substituted this gives

$$C_f = \frac{16}{3R}g_1(0). \tag{29}$$

The pressure drag coefficient is

$$C_p = -\frac{1}{\rho U_\infty^2}\int_0^\pi p(0,\theta)\sin 2\theta\, d\theta,$$

where $p(\xi,\theta)$ is the pressure in the fluid. From the equations of motion it may be shown that

$$\left(\frac{\partial p}{\partial\theta}\right)_{\xi=0} = \frac{\rho\nu U_\infty}{a}\left(\zeta+\frac{\partial\zeta}{\partial\xi}\right)_{\xi=0}, \tag{30}$$

and if we integrate with respect to θ and then substitute in the preceding integral, we obtain

$$C_p = -\frac{8}{3R}\{g_1(0)+g_1'(0)\}. \tag{31}$$

The surface pressure is expressed in terms of a dimensionless pressure coefficient. First, by integrating the appropriate equation of motion along the axis $\theta = \pi$ from $\xi = 0$ to $\xi = \infty$, the pressure coefficient

$$k(\pi) = \frac{p_\pi - p_\infty}{\frac{1}{2}\rho U_\infty^2} = 1+\frac{8}{R}\int_0^\infty \left(\frac{\partial\zeta}{\partial\theta}\right)_{\theta=\pi} d\xi \tag{32}$$

is obtained. Here, p_π is the pressure at $\theta = \pi$ on the equator of the sphere and p_∞ is the uniform pressure at infinite distance from the sphere. Finally, on integration of the result (30) around the equator of the sphere, the pressure coefficient at angular co-ordinate θ is obtained in the form

$$k(\theta) = \frac{p-p_\infty}{\frac{1}{2}\rho U_\infty^2} = k(\pi)+\frac{4}{R}\int_\pi^\theta \left(\frac{\partial\zeta}{\partial\xi}+\zeta\right)_{\xi=0} d\theta. \tag{33}$$

R	C_f	C_p	C_D	$k(0)$	$k(\pi)$
0·1	81·40	40·70	122·10	−60·07	62·03
0·2	41·34	20·67	62·02	−30·05	31·97
0·5	17·23	8·622	25·85	−12·02	13·86
0·8	11·17	5·598	16·76	−7·516	9·289
1	9·134	4·585	13·72	−6·017	7·753
5	2·369	1·236	3·605	−1·203	2·599
10	1·427	0·785	2·212	−0·654	1·878
20	0·854	0·512	1·365	−0·322	1·471
40	0·536	0·368	0·904	−0·192	1·261

TABLE 4. Physical properties of the solutions

Calculated drag coefficients are given in table 4 together with values of $k(0)$ and $k(\pi)$. These agree well with the calculated results of Le Clair *et al.* (1970). The coefficient C_D is compared with the results of other numerical investigations in table 5 and the quantity $(D/D_s)-1$, where D is the drag and D_s is the Stokes drag, is compared with theory and experimental results in figure 1. Two sources of experimental measurements have been used in figure 1. The first are the results of Maxworthy (1965) and the second are several sets of measurements recently correlated by Pruppacher *et al.* (1970). These latter measurements have been placed on a curve by these authors and are presented here in this manner. The present results appear to agree very well with experiment.

R	Jenson (1959)	Dennis & Walker (1964)	LeClair, Hamielec & Pruppacher (1970)†	Rimon & Cheng (1969)	Present results
0·1	—	—	122·04	—	122·10
1	—	13·5	13·66	—	13·72
5	3·98	—	3·515	—	3·605
10	2·42	2·06	2·144	2·205	2·212
20	1·473	1·32	1·356	—	1·365
40	0·930	—	0·930	0·930	0·904

(† These values are half the values quoted by Le Clair *et al.* (1970) who define $C_D = D/(\frac{1}{2}\pi\rho a^2 U_\infty^2)$)

TABLE 5. Comparison of C_D

Comparison of the present results for C_D in the range $R = 0{\cdot}1$ to 1 may also be made with the results of the asymptotic theories for low R. A recent paper by Chester & Breach (1969) has shown that the method of matched asymptotic expansions gives the result

$$C_D = \frac{12}{R}\{1+\tfrac{3}{16}R+\tfrac{9}{160}R^2[\log\tfrac{1}{2}R+\gamma+\tfrac{5}{3}\log 2-\tfrac{323}{360}]+\tfrac{27}{640}R^3\log\tfrac{1}{2}R+O(R^3)\}, \tag{34}$$

where γ is Euler's constant. The expansion is valid as $R\to 0$ and the terms up to and including the term in $R^2\log\frac{1}{2}R$ inside the braces were given by Proudman & Pearson (1957). Maxworthy (1965) has suggested that the expression

$$C_D \approx \frac{12}{R}(1+\tfrac{3}{16}R-\tfrac{19}{1280}R^2+\tfrac{71}{20480}R^3), \tag{35}$$

given by Goldstein (1929) on the basis of Oseen theory is as good as any for calculating the drag for $R < 0{\cdot}9$. The same conclusion cannot be drawn from the comparison of the present results with the theories given over the range $R = 0{\cdot}1$ to 1 in table 6. The present results are also illustrated for $R \leqslant 1$ in figure 1(*b*). They indicate that the expression of Chester & Breach (1969) gives a better approximation to the drag coefficient than any other asymptotic solution until about $R = 0{\cdot}6$. The calculated values of C_D lie between the curves of Proudman &

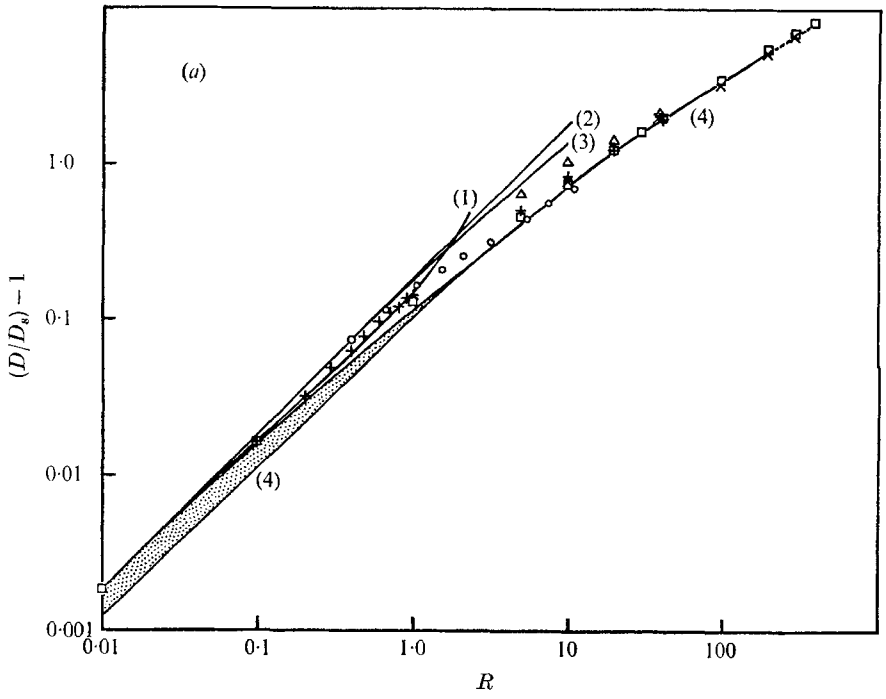

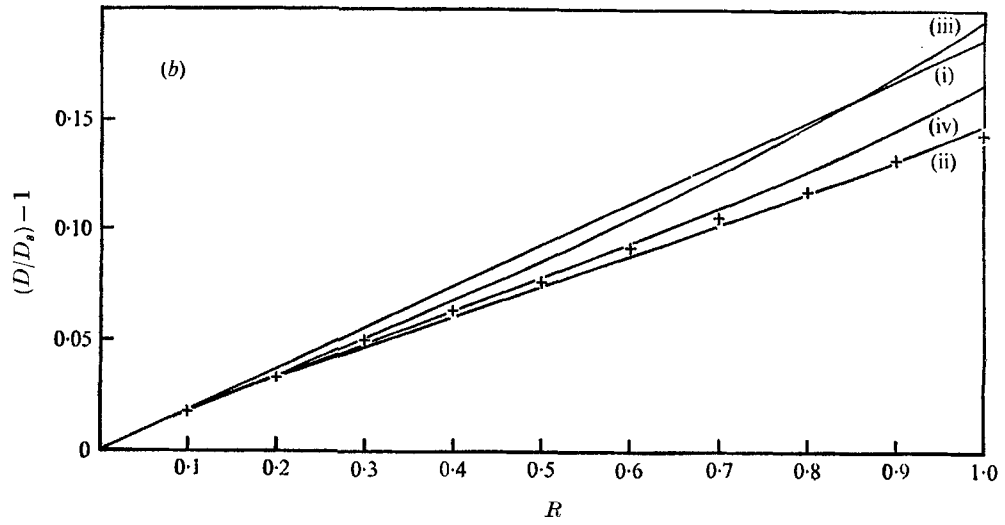

FIGURE 1. (*a*) Comparison with theory and experiment, $(D/D_s)-1$: (1), Proudman & Pearson; (2), Oseen; (3), Goldstein; (4), Pruppacher–Steinberger, Pruppacher, Beard–Pruppacher (experimental); ▦ experimental scatter; ○, Maxworthy (experimental); □, Le Clair, Hamielec & Pruppacher; △, Jenson; ×, Rimon & Cheng; +, present results. (*b*) Comparison with theory:

(i) Oseen $\dfrac{D}{D_s}-1=\dfrac{3R}{16}$;

(ii) Proudman & Pearson $\dfrac{D}{D_s}-1=\dfrac{3R}{16}+\dfrac{9}{160}R^2\log\tfrac{1}{2}R$;

(iii) Chester & Breach $\dfrac{D}{D_s}-1=\dfrac{3R}{16}+\dfrac{9R^2}{160}[\log\tfrac{1}{2}R+\gamma+\tfrac{5}{3}\log 2-\tfrac{323}{360}]$;

(iv) Chester & Breach $\dfrac{D}{D_s}-1=\dfrac{3R}{16}+\dfrac{9R^2}{160}[\log\tfrac{1}{2}R+\gamma+\tfrac{5}{3}\log 2-\tfrac{323}{360}]+\dfrac{27R^3}{640}\log\tfrac{1}{2}R$.

Pearson (1957) and Chester & Breach (1969). As R increases they gradually coincide at $R = 0{\cdot}8$ and $0{\cdot}9$ with the Proudman & Pearson (1957) expression. Thereafter ($R \geqslant 1$) all theories progressively overestimate the drag. This is in agreement with the conclusions of Le Clair *et al.* (1970) and Pruppacher *et al.* (1970), that as the Reynolds number approaches zero, the drag approaches the Stokes drag in the above manner rather than via the Oseen drag as the experimental results of Maxworthy (1965) suggested.

R	Goldstein	Proudman–Pearson	Chester–Breach	Present results
0·1	122·23	122·05	122.09	122·10
0·2	62·22	61·94	62·01	62·02
0·3	42·20	41·87	41·95	42·02
0·4	32·19	31·82	31·91	31·91
0·5	26·17	25·78	25·88	25·85
0·6	22·16	21·76	21·88	21·85
0·7	19·29	18·90	19·03	18·96
0·8	17·13	16·76	16·91	16·76
0·9	15·46	15·10	15·28	15·10
1·0	14·11	13·78	14·00	13·72

TABLE 6. Comparison of C_D with theory for low R

Streamlines and equi-vorticity lines for the flow are shown over the range $R = 1$ to 40 in figures 2 and 3, respectively. The variation of the vorticity over the equator of the sphere is shown for the same range of R in figure 4. One of the main points of interest is to determine the Reynolds number at which a separated wake first appears behind the sphere and to examine the subsequent development of the wake with Reynolds number. Various authors, including Kawaguti (1950), Lister (1953), Dennis & Walker (1964) and Hamielec *et al.* (1967) have found that separation has not started to occur before $R = 20$. Jenson (1959) has estimated that separation starts at $R = 17$ and Rimon & Cheng (1969) obtained a separated flow for R as low as 10. The present solutions indicate that separation of the flow has not started at $R = 20$. Separation first starts when $\partial\zeta/\partial\theta$ becomes zero at the point $\xi = 0$, $\theta = 0$. A linear interpolation between the values of $\partial\zeta/\partial\theta$ at this point for the cases $R = 20$ and $R = 40$ gives an estimate $R = 20{\cdot}5$ for the onset of separation. This prediction is in excellent agreement with the results of Le Clair *et al.* (1970) and Pruppacher *et al.* (1970) who estimate separation starts at $R = 20$.

Separated flow past a sphere has been studied experimentally by Taneda (1956). He has found that separation starts somewhere between $R = 22$ and $R = 25$ and has estimated $R = 24$ as giving the start of separation, although the precise onset was difficult to observe. Taneda (1956) has also measured the growth of the length of the separated region behind the sphere as a function of Reynolds number. The present calculation at $R = 40$ gives the length of this region, measured along the axis $\theta = 0$ from the rearmost point of the sphere, as 0·30 diameters. This value lies between the estimates of about 0·24 diameters of Jenson (1959) and 0·33 of Rimon & Cheng (1969), and appears to give a very close

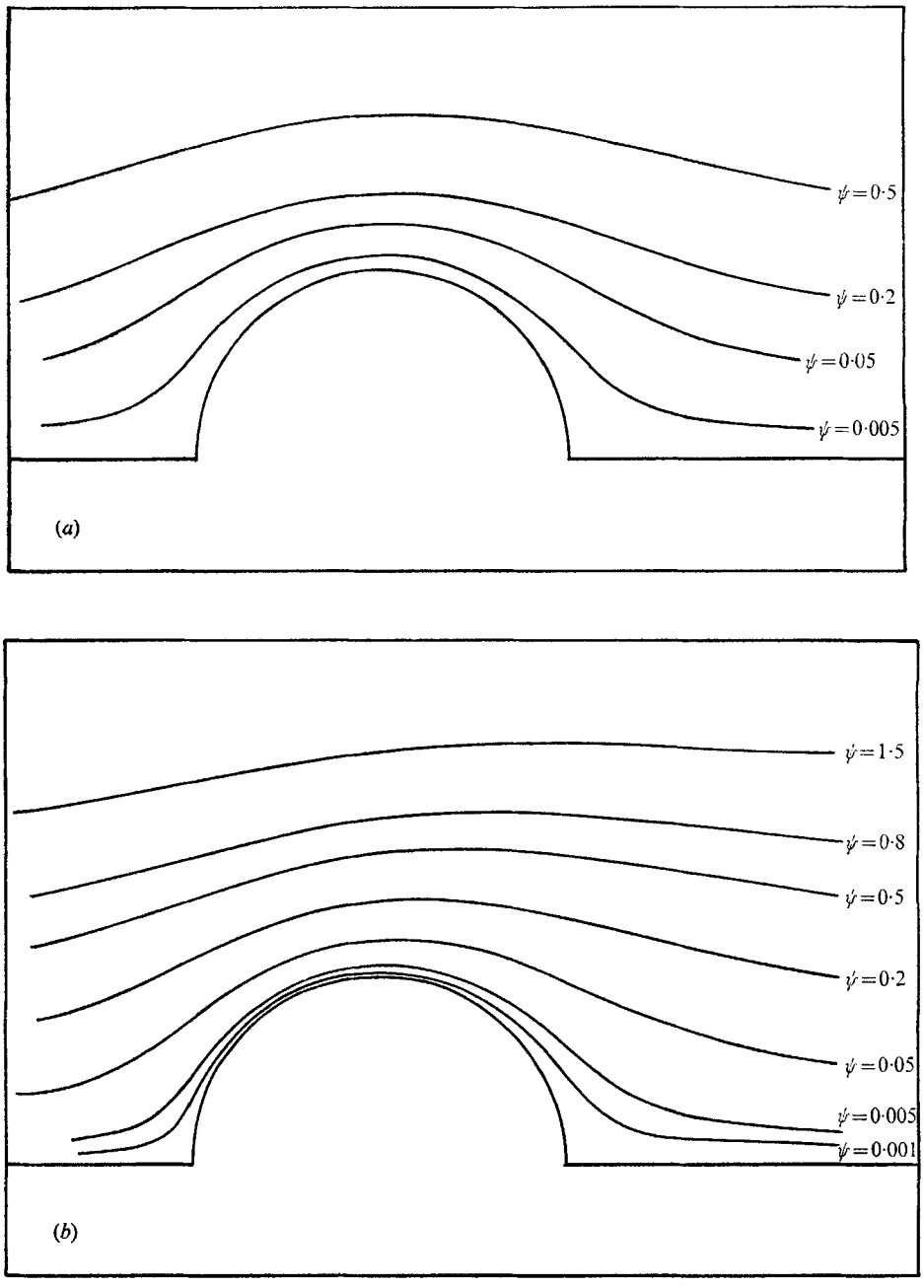

FIGURE 2. For legend see facing page.

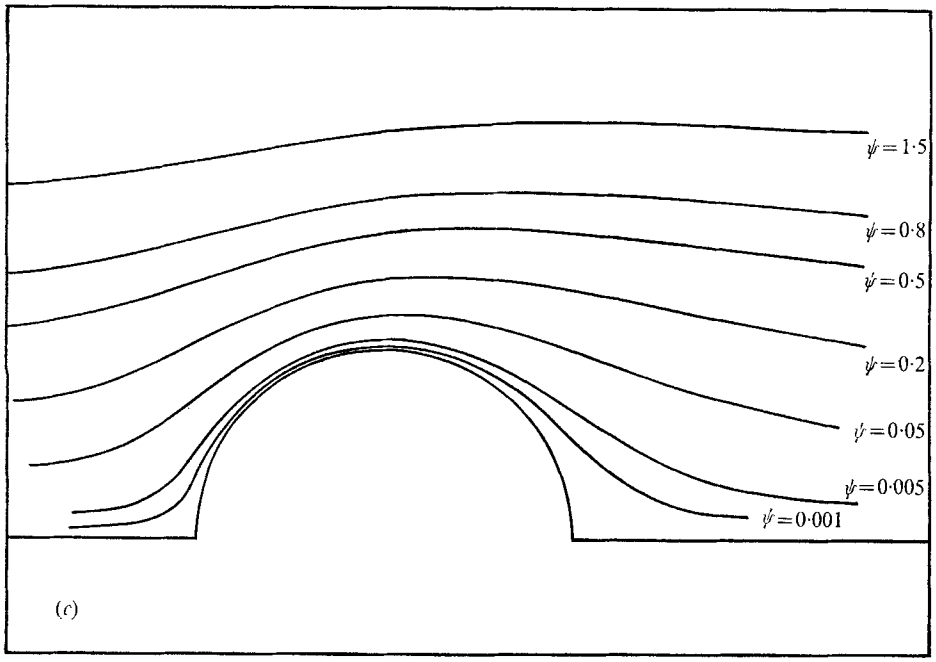

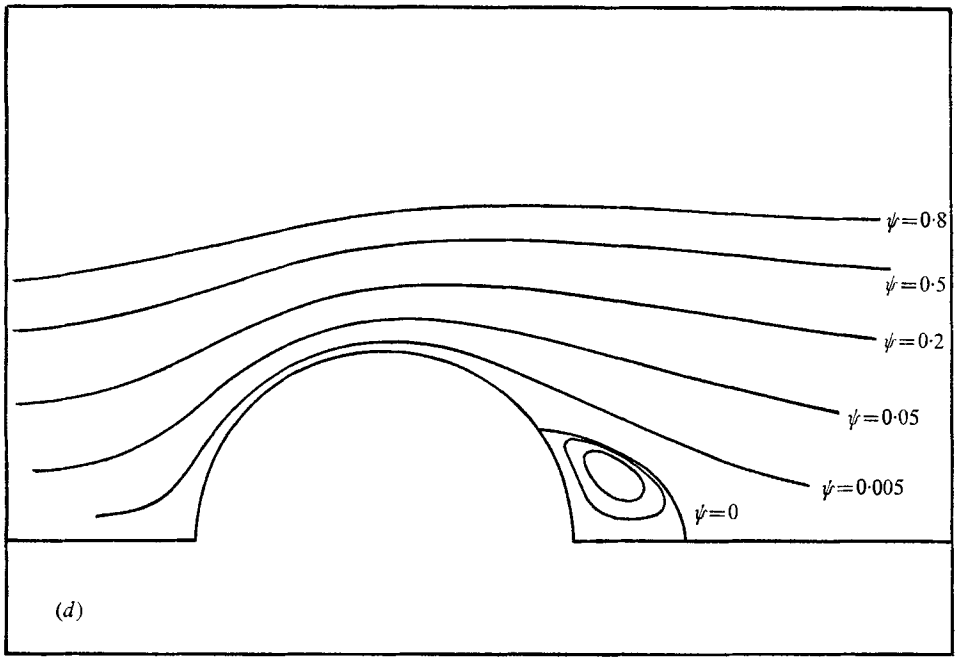

FIGURE 2. Streamlines for: (*a*) $R = 1$, (*b*) $R = 10$, (*c*) $R = 20$, (*d*) $R = 40$ (enclosed streamlines, starting from the centre, are $\psi = -0{\cdot}0003$ and $\psi = -0{\cdot}0001$).

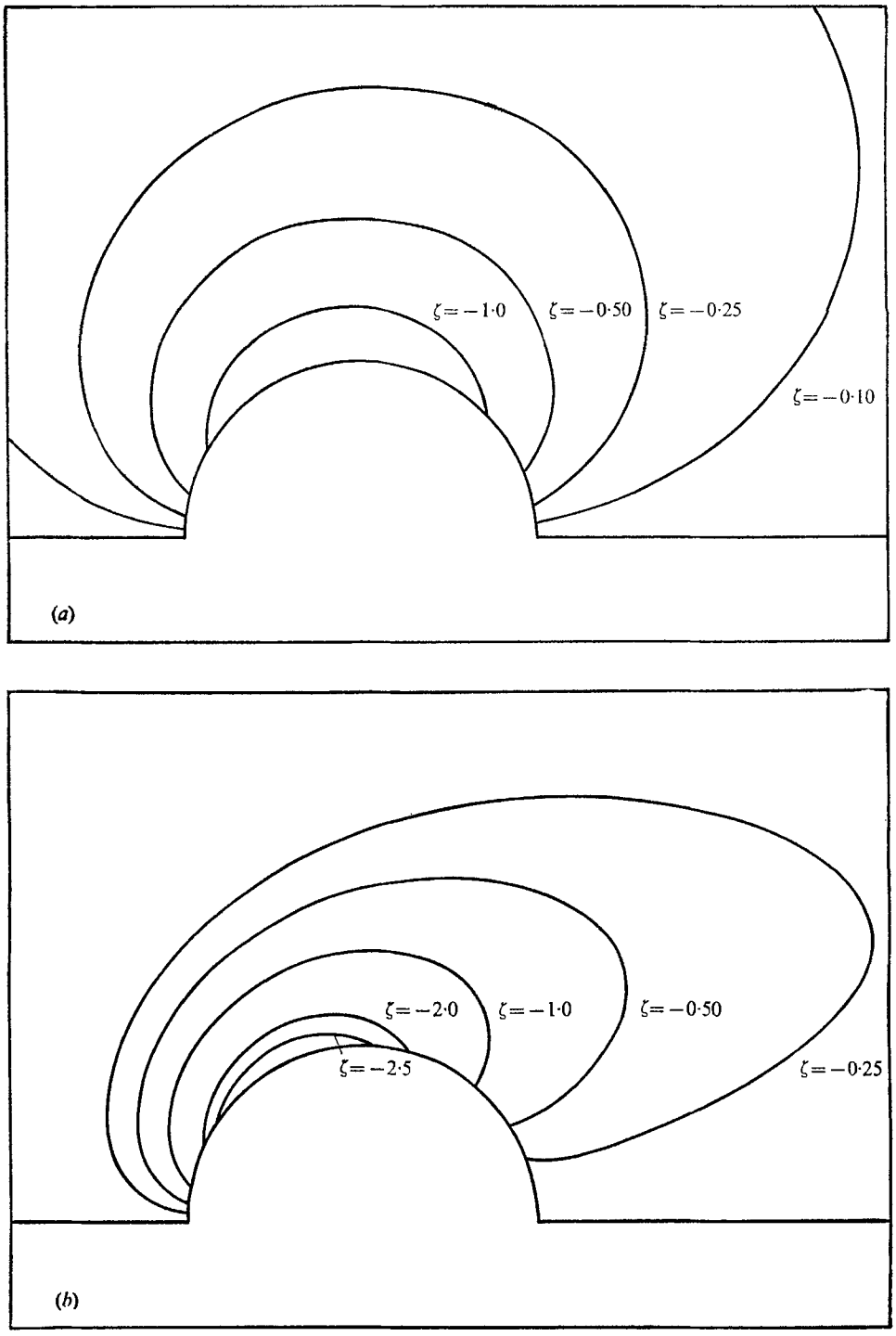

FIGURE 3. For legend see facing page.

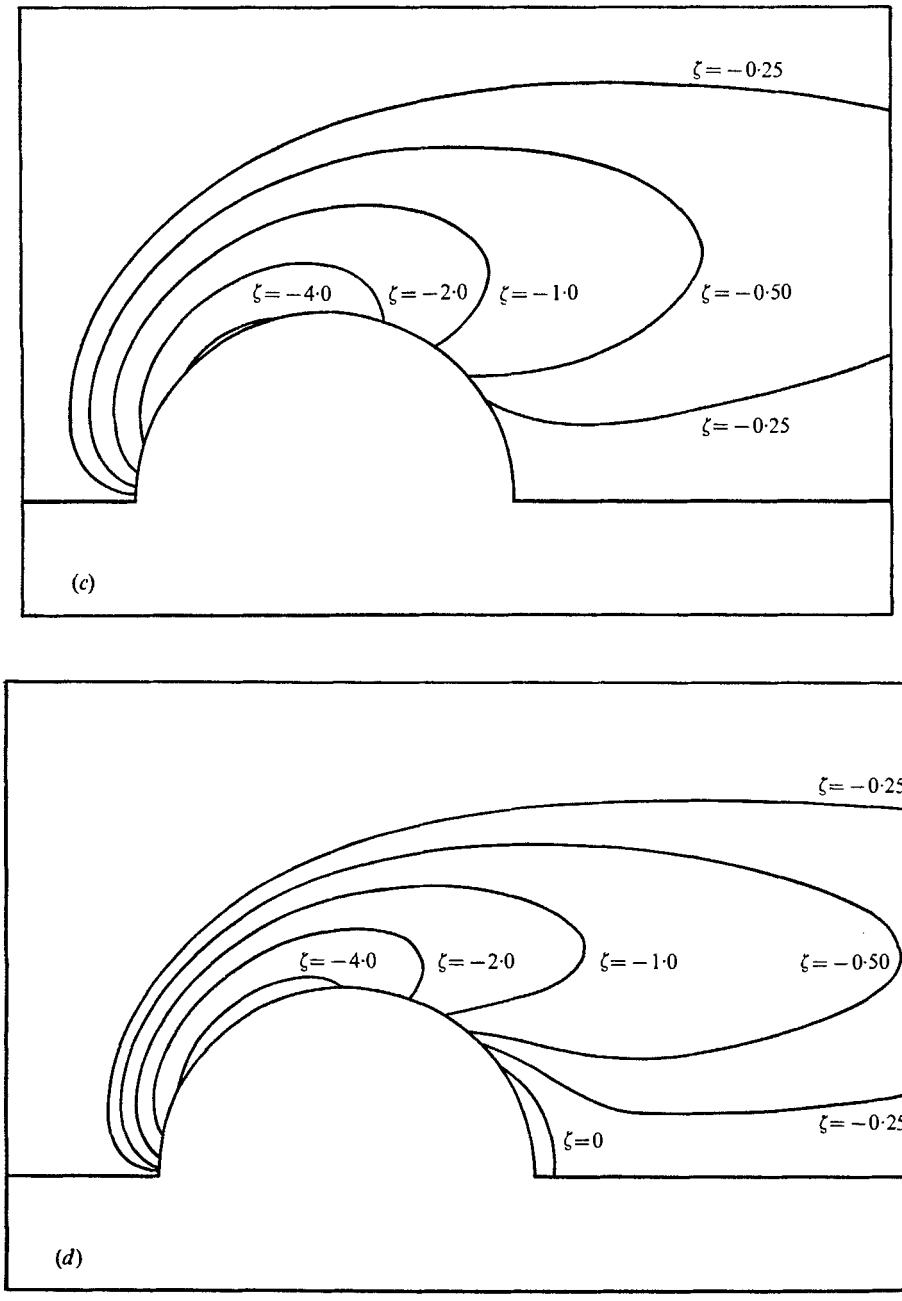

FIGURE 3. Equi-vorticity lines for: (*a*) $R = 1$, (*b*) $R = 10$, (*c*) $R = 20$, (*d*) $R = 40$.

fit with the experimental result. This result also agrees well with the calculated eddy length of Le Clair *et al.* (1970) and Pruppacher *et al.* (1970) for $R = 40$.

One further check of the present results with theory may be obtained by comparing the tendency of the pressure coefficient $k(\pi)$ at the front stagnation point as R increases with the result

$$k(\pi) \sim 1 + \frac{12}{R + 0{\cdot}643R^{\frac{1}{2}}}, \tag{36}$$

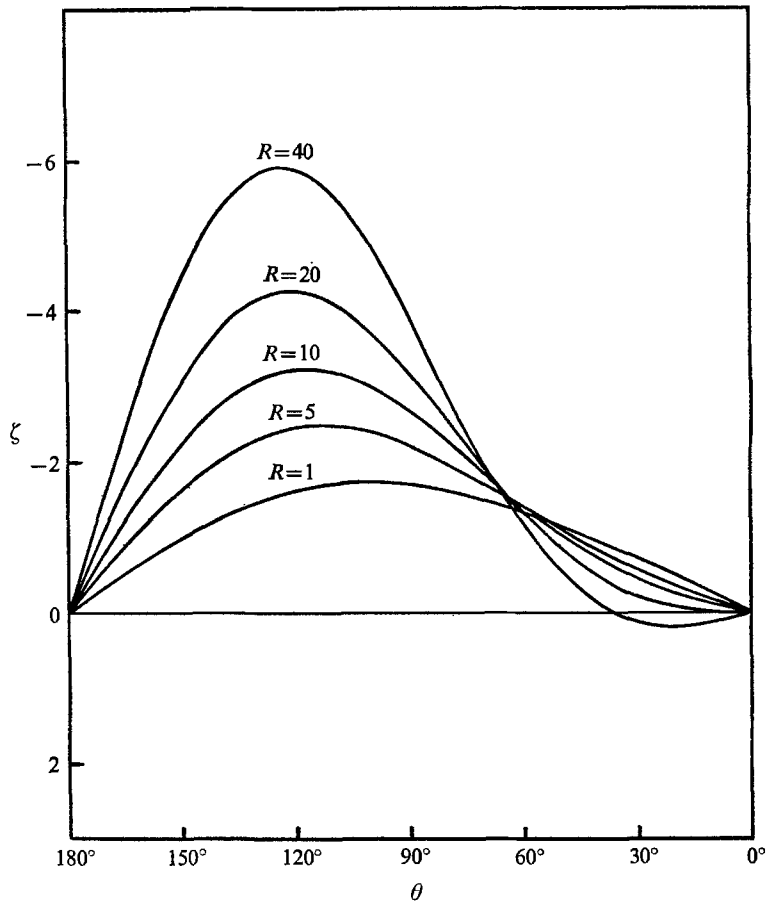

FIGURE 4. Vorticity distribution over the surface of the sphere.

obtained by Homann (1936) from boundary-layer theory. It is found that the calculated values in table 4 steadily approach the values given by (36) with increasing R. The discrepancy is less than 4 % at $R = 20$ and less than 1 % at $R = 40$. The present calculations of $k(\pi)$ are consistently lower than those of Jenson (1959) over the range $R = 5$ to 40, but there is reasonable agreement in the shape of the pressure distributions over the equator of the sphere. Pressure distributions over the equator of the sphere are given for the range $R = 5$ to 40 in figure 5. The precise details of $k(\theta)$ can be calculated for the whole range of R from the results given in tables 2 and 3.

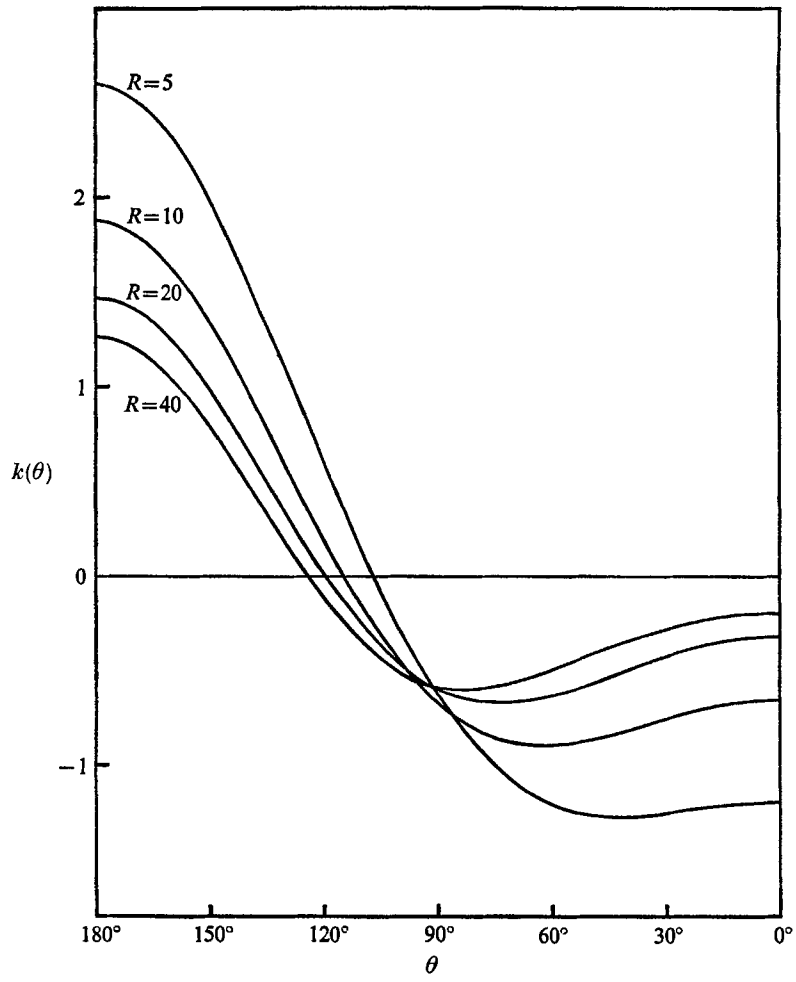

FIGURE 5. Pressure distribution over the surface of the sphere for $R = 5, 10, 20, 40$.

5. Discussion

The main advantages of the series truncation method arise from the fact that the problem is reduced to the solution of ordinary differential equations. First, the necessity of approximating derivatives in the θ direction by finite differences is avoided. This is known to present difficulties in the far wake region behind the body. Secondly, it is possible to use a small grid size h with a reasonably large field length l without encountering the practical difficulties imposed by computer core limitations when methods based on two-dimensional finite differences are used. The method does, however, introduce the problem of the maximum number of modes n_0 which must be used to obtain an accurate approximation for a given Reynolds number.

The number of modes required increases rapidly with R and the present calculations were terminated at $R = 40$ with $n_0 = 20$. Although this range could be

extended further, K would certainly have to be taken less than that value used for $R = 40$. Since K must not be taken too small relative to the exit tolerance ϵ, in order to maintain a realistic iterative scheme, it is felt that this method has been pursued to approximately its upper limit at $R = 40$.

n_0	$g_1(0)$	$g_2(0)$	$g_3(0)$	$g_4(0)$	C_D
10	2·7210	−0·7231	0·0050	0·0008	2·246
12	2·6879	−0·7136	0·0060	0·0010	2·222
14	2·6791	−0·7091	0·0056	0·0013	2·215
16	2·6764	−0·7075	0·0053	0·0014	2·212
Estimates	2·6752	−0·7066	0·0044	0·0014	2·210

TABLE 7. Effect of truncation on the solution for $R = 10$

The effect of variation of n_0 on the solutions has been studied. For $R \leqslant 1$, taking n_0 greater than 6 produces no change in the solutions. For $R > 1$, some typical results are shown for the case $R = 10$ in table 7. Although it cannot be said that the results have completely converged when $n_0 = 16$, it is unlikely that much further change will take place as n_0 is increased. Underwood (1969) has suggested that it may be possible to estimate the effect of increasing the order of the truncation by applying the extension of Shanks (1955). If T_{n-1}, T_n, T_{n+1} are three successive approximations to a quantity, a revised estimate is given by

$$T \approx \frac{T_{n+1}T_{n-1} - T_n^2}{T_{n+1} + T_{n-1} - 2T_n}. \tag{37}$$

This scheme has been applied to the results for $n_0 = 12, 14$ and 16 in table 7 to give the estimates shown in the final row of the table. The physical properties derived from this estimated solution are all found to be considerably less than 1 % different from those which have been derived from the solution for $n_0 = 16$ and which were given in the previous section. Similar remarks apply to the other Reynolds numbers for $R > 1$ and all the results given in the previous section are thought to be correct to within 1 %.

This work was supported by a grant from the National Research Council of Canada.

REFERENCES

BATCHELOR, G. K. 1967 *An Introduction to Fluid Dynamics*. Cambridge University Press.

BEARD, K. V. & PRUPPACHER, H. R. 1969 *J. Atmos. Sci.* **26**, 1066.

CASTLEMAN, R. A. 1926 *N.A.C.A. Tech. Note* no. 231.

CHESTER, W. & BREACH, D. R. 1969 *J. Fluid Mech.* **37**, 751.

DENNIS, S. C. R. & CHANG, G. Z. 1969 *Mathematics Research Center, University of Wisconsin. Technical Summary Report* no. 859.

DENNIS, S. C. R. & WALKER, M. S. 1964 *Aero. Res. Counc.* no. 26, 105.

GOLDSTEIN, S. 1929 *Proc. Roy. Soc.* A **123**, 225.

GOLDSTEIN, S. 1938 *Modern Developments in Fluid Dynamics*. Oxford University Press.

HOMANN, F. 1936 *N.A.C.A. Tech. Mem.* no. 1334.

HAMIELEC, A. E., HOFFMAN, T. W. & ROSS, L. L. 1967 *A.I.Ch.E.J.* **13**, 212.

JENSON, V. G. 1959 *Proc. Roy. Soc.* A **249**, 346.

KAWAGUTI, M. 1950 *Rep. Inst. Sci. Tokyo*, **4**, 154.

LE CLAIR, B. P., HAMIELEC, A. E. & PRUPPACHER, H. R. 1970 *J. Atmos. Sci.* **27**, 308.

LISTER, M. 1953 Ph.D. Thesis, London.

MAXWORTHY, T. 1965 *J. Fluid Mech.* **23**, 369.

OSEEN, C. W. 1910 *Ark. f. Mat. Astr. og Fys.* **6**, 29.

PERRY, J. 1950 (ed.) *Chem. Engng Handbook*, 3rd ed. New York: McGraw-Hill:

PROUDMAN, I. & PEARSON, J. R. A. 1957 *J. Fluid Mech.* **2**, 237.

PRUPPACHER, H. R., LE CLAIR, B. P. & HAMIELEC, A. E. 1970 *J. Fluid Mech.* **44**, 781.

PRUPPACHER, H. R. & STEINBERGER, E. H. 1968 *J. Appl. Phys.* **39**, 4129.

RIMON, Y. & CHENG, S. I. 1969 *Phys. Fluids*, **12**, 949.

ROSSER, J. B. 1967 *Mathematics Research Center, University of Wisconsin, Technical Summary Report* no. 797.

ROTENBERG, M., BIVINS, M., METROPOLIS, N. & WOOTEN, J. K. 1959 *The 3-j and 6-j Symbols*. Massachusetts Institute of Technology Press.

SCHLICHTING, H. 1960 *Boundary Layer Theory* (4th ed.). New York: McGraw-Hill.

SHANKS, D. 1955 *J. Math. Phys.* **34**, 1.

TALMAN, J. D. 1968 *Special Functions*. New York: Benjamin.

TANEDA, S. 1956 *J. Phys. Soc. Japan*, **11**, 302.

UNDERWOOD, R. L. 1969 *J. Fluid Mech.* **37**, 95.

VAN DYKE, M. D. 1964*a* *Proc. 11th Int. Cong. Appl. Mech.*, Munich, 1165–1169.

VAN DYKE, M. D. 1964*b* *Perturbation Methods in Fluid Mechanics*. New York: Academic.

VAN DYKE, M. D. 1965 *Stanford University SUDAER* no. 247.

WALKER, J. D. A. 1968 M.Sc. Thesis, University of Western Ontario.